

Effect of Reinforcement on Early-Age Cracking in High Strength Concrete

M. S. Sule¹ and K. van Breugel²

¹ Dutch Ministry of Transport, Public Works and Water Management (RWS),
Road and Hydraulic Engineering Division, The Netherlands*

² Faculty of Civil Engineering and Geosciences, Delft University of Technology, Delft,
The Netherlands

During hydration, high strength concrete (HSC) is subjected not only to thermal effects but also to load-independent deformations, i.e. autogenous shrinkage. The additional autogenous shrinkage makes hardening HSC prone to cracking. As the prediction of the probability of cracking is solely based on the behaviour of concrete it was found that this is sometimes too pessimistic for reinforced HSC-structures. In order to investigate the stress development and the probability of cracking in hardening reinforced HSC, a Temperature Stress Testing Machine (TSTM) has been used for simulating the mechanical boundary conditions and for imposing different curing temperatures onto concrete specimens. The specimens were made of HSC and normal strength concrete (NSC). They were reinforced with different reinforcement percentages (0%, 0.75%, 1.34% and 3.02%) and configurations (one reinforcement bar and four reinforcement bars). It was found that four rebars in the corners of the test specimen postpone the moment of through-cracking, whereas specimens with one centrally placed rebar cracked almost as sudden as plain specimens. For quantifying the effect of reinforcement on the moment of cracking due to restrained load-independent deformations, a "strain enhancement factor" has been introduced. By applying the strain enhancement factor, the cracking probability of a reinforced HSC-structure can be estimated more realistically at early-age.

Keywords: Early-age cracking, high strength concrete

1 The problem to predict early-age cracking in reinforced high strength concrete structures

1.1 Background

The development of high strength concrete (HSC) meets the steadily increasing demands on building higher, more slender, faster etc. A positive side effect is the dense microstructure of HSC. This property is interesting for all kind of structures (bridges, tanks etc.) that have to meet high durability demands especially in aggressive environments.

* The research was carried out at Delft University of Technology as part of a PhD study.

Unfortunately, HSC also has a disadvantage. It is prone to early-age cracking. Therefore a lot of research has been done to predict the probability of cracking of hardening HSC. However, in practice it has been observed that reinforced HSC-structures are sometimes less sensitive to early-age cracking than expected. The question is therefore:

How prone are reinforced HSC-structures really to early-age cracking?

Or, in other words:

How does reinforcement affect the probability of cracking?.

In order to judge the probability of cracking of hardening concrete structures both temperature criteria (as discussed by *Emborg and Bernander 1994*) and stress criteria (*Lokhorst 2001*) are used in practice. Therefore temperature differences are limited in a structure or shrinkage reducing agents are added to the concrete mixtures to reduce autogenous shrinkage strains and consequently slow down the stress development and reduce the resulting stresses.

In order to control early-age cracks a crack distributing reinforcement is applied. This reinforcement distributes cracks and consequently reduces their widths. As a result a large number of smaller cracks form instead of a few through-cracks. This means that due to the formation of fine cracks the strain capacity of a reinforced concrete element can be increased before the occurrence of through-cracks. However, this positive effect of reinforcement has not been quantified up to now for hardening concrete. An adequate criterion for judging the “strain enhancing effect” of reinforcement might best be taken into account with a strain criterion.

In order to determine a minimum reinforcement ratio needed to postpone the occurrence of through-cracks and to control crack widths at early-age, the bond behaviour between hardening concrete and reinforcement steel has to be known. Up to now, crack width calculations have been based on bond behaviour between hardened concrete and reinforcing steel. It is not known if these existing models can also be applied to hardening concrete, especially hardening HSC.

The above mentioned uncertainties about the behaviour of reinforced HSC-structures during the hardening phase may lead to conservative assumptions for the determination of the required reinforcement ratios.

1.2 Point of departure

The stress development and the probability of cracking in early-age concrete has been investigated by different researchers. In order to simulate stress development due to restrained early-age deformations, a Temperature Stress Testing Machine (TSTM) has been built at Delft University of Technology (*Lokhorst 2001*). For the here reported research there was no need to adapt or change this set-up.

In literature bond stress-slip relationships always refer to hardened concrete. Knowing that bond stress depends, among other things, on the strength development of concrete, a bond stress-slip

relationship had to be found that accounts for this development. This was done with the help of pull-out tests. The experiments and their results are not discussed here but in *Sule & Van der Veen (2002)*.

2 Experimental research on stress development and cracking behaviour of reinforced concrete

2.1 Aim of the experimental research

The aim of the experiments performed in this study is to give more information about how reinforcement affects the stress development and the cracking behaviour of a specimen subjected to restrained early-age deformations. For this purpose experiments were performed on sealed concrete specimens in the laboratory in order to measure exclusively thermal and autogenous deformations. Drying shrinkage is not considered, since it hardly plays a role for through-cracking at very early ages (plastic shrinkage ignored). The observed behaviour of early-age reinforced concrete specimens serves to predict stress development and the moment of cracking.

2.2 Types of experiments

The development of concrete properties has to be known to quantify stress development due to restrained early-age deformations. Therefore cube compressive strength and the E-modulus have been tested. The results are discussed by the author in *Sule 2003*. In order to get more information about the development of bond strength pull-out tests were performed (*Sule & Van der Veen 2002*). Furthermore the load-independent deformations of a plain and a reinforced specimen have been measured giving an indication of the restraining effect of reinforcement on the free deformation. Last but not least the stress development and the moment of cracking of a reinforced specimen were obtained from the measurements in the Temperature Stress Testing Machine (TSTM). In Table 1 the tested reinforcement diameters (6, 8, 12, 16, 25 mm) and configurations (one and four rebars) are summarized. Due to the limited load capacity of the TSTM, the concrete cross section had to be reduced for HSC (from originally 150 x 150 mm² to 150 x 100 mm²). This explains the difference of the reinforcement ratios used in NSC and HSC (Table 1). Four reinforcing bars were placed in the corners of the specimen with a concrete cover of 20 mm. One reinforcing bar was placed centrally in the cross section.

Table 1: List of experiments performed in the TSTM.

concrete composition	cross section [mm ²]	reinforcement configuration	reinforcement ratio [%]	temperature development
HSC	150x100	-	-	semi-ad.(2 tests), 20°C, 40°C
HSC	150x100	1Ø12	0.76	semi-ad., 20°C
HSC	150x100	4Ø6	0.76	semi-ad., 20°C
HSC	150x100	1Ø16	1.36	semi-ad., 20°C, 30°C, 40°C
HSC	150x100	4Ø8	1.36	semi-ad.(3 tests), 20°C, 30°C, 40°C
HSC	150x100	1Ø25	3.38	semi-ad., 20°C
HSC	150x100	4Ø12	3.11	semi-ad. (3 tests), 20°C
NSC	150x150	-	-	semi- ad.
NSC	150x150	1Ø16	0.90	semi- ad.
NSC	150x150	4Ø8	0.90	semi- ad.
NSC	150x150	1Ø25	2.23	semi- ad.
NSC	150x150	4Ø12	2.05	semi- ad.

2.3 Experimental programme

2.3.1 Material

In this research project a NSC and a HSC have been investigated. The mixtures, given in Table 2, were chosen from earlier research projects for two reasons. Firstly, in order to see if experiments are well reproducible and secondly in order to refer to the concrete properties investigated earlier (*Sule et al. 2000*).

Lokhorst (2001) investigated NSC with Portland and Blast furnace slag cement and different w/c-ratios. This concrete mixture (P-05), based on Portland cement with a w/c-ratio of 0.5, is also used in this research project. *Koenders (1997)* investigated, among other things, the behaviour of a HSC (B85 called *spobmod_2*) with a w/c-ratio of 0.33 that was used in an in-situ cast cantilever bridge.

Table 2: Concrete compositions in kg/m³.

	NSC	HSC
	kg/m ³	kg/m ³
Water	175.0	125.4
CEM III/ B 42.5 LH HS	-	237.0
CEM I 52.5 R	-	238.0
CEM I 32.5 R	350.0	-
Slurry microsilica (50/50)	-	50.0
Superplasticizer BV1(based on lignosulfanate)	-	1.0
Superplasticizer FM951(based on naftaleensulfanate)	-	9.5
Gravel 4 - 16 mm	-	973.5
Gravel 4 - 8 mm	827.6	-
Sand 0 - 4 mm	1011.5	796.5

In the experiments, use was made of hot rolled ribbed reinforcing steel FeB 500 HWL.

2.3.2 Curing temperature

All specimens were poured from the same batch of concrete and were cured under the same conditions: isothermal (20°C, 30°C, 40°C) or semi-adiabatic.

Semi-adiabatic curing conditions are often also known as “realistic” curing conditions. The temperature develops freely due to the hydration process similar to the temperature development in real structures. Figure 1 shows the characteristic semi-adiabatic temperature developments measured in NSC (left) and HSC (right) which generate thermal deformations of the specimens.

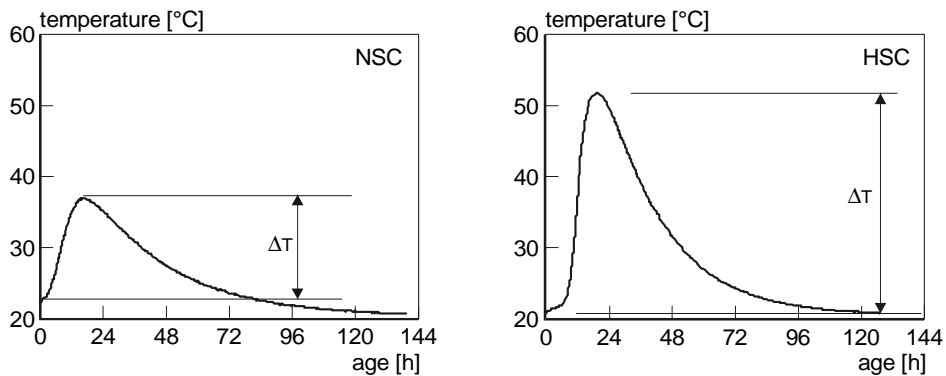


Figure 1: Temperature development of NSC (left) and HSC (right) under semi-adiabatic curing.

HSC undergoes additional autogenous deformations which can be exclusively registered under curing at a constant temperature (isothermal curing).

In order to obtain the desired temperature history all specimens were cast in temperature controlled moulds which were controlled by five cryostats connected to a personal computer. In a closed loop control the temperature of the water in a cryostat was adjusted to the required temperature. For the semi-adiabatic curing condition the temperature development was measured in *one* specimen and was then imposed onto the other specimens. Consequently the hydration process in all specimens developed at the same rate. This ensured that properties measured in the experiments related to the same degree of hydration. In isothermally cured experiments the temperatures of *all* specimens were controlled directly by the PC.

2.4 Experimental set-up

2.4.1 Measuring self-induced stresses in the TSTM

The Temperature Stress Testing Machine (TSTM) is a horizontal steel frame in which hardening concrete specimens can be loaded in compression and in tension under various hardening conditions (Figure 2, *Lokhorst, 2001*). With the help of temperature controlled moulds any thermal condition can be realised. Both load-controlled and deformation-controlled experiments can be performed.

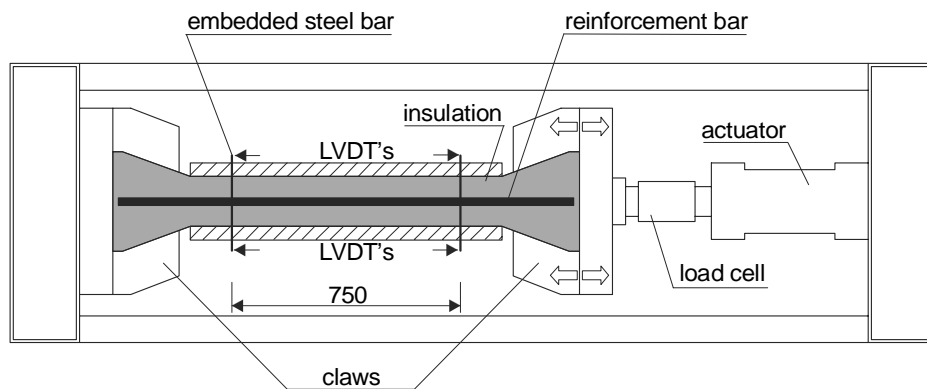


Figure 2: The Temperature Stress Testing Machine (top view - schematic).

In this research work all TSTM-experiments were fully restrained. Therefore the measuring distance of 750 mm was kept constant. Depending on the concrete deformations, compressive and tensile forces had to be applied to adjust the measuring distance. This is realised with help of an hydraulic actuator. The specimen is hold with a dovetailed interlock between the concrete specimen and the frame. Two steel claws hold the dovetailed specimen. One of the claws is fixed to the frame, the other lies on roller-bearings and can be moved with a hydraulic actuator. The claws are pre-stressed to avoid slip of the specimen if the load changes from compression to tension.

As shown in Figure 2 the specimen was cast in a combined mould that consisted of an insulated temperature controlled mould for the middle part of the specimen and the claws surrounding the two ends of the specimen. A short formwork was fixed to the claws. This formwork formed a smooth transition between the straight insulated mould and the slanting inner sides of the claws. Originally, the cross section of the specimen was 150 x 150 mm². As the capacity of the machine was limited to 100 kN in compression and tension this cross section had to be reduced for testing the cracking behaviour of HSC at early-age. The cross section of HSC specimens was therefore 150 x 100 mm².

The measurements started as soon as concrete had sufficient stiffness. This varied from 5 to 12 hours after mixing depending on the concrete mixture and hardening temperature.

2.4.2 Measuring load-independent deformations in the ADTM

The load-independent deformations during hardening have been determined with unrestrained specimens. This set-up is also called the Autogenous Deformation Testing Machine (ADTM). In this research project two ADTMs were used. In the first ADTM a plain specimen was tested and in the second a reinforced one. In the latter it was investigated how reinforcement influences load-independent deformation.

The inner dimensions of the ADTM-mould was 1000 mm x 150 mm x 150 mm (length, width, height) for a plain specimen. The free deformation of a reinforced specimen was measured at a specimen with cross section of 150 mm x 150 mm for NSC and 150 mm x 100 mm for HSC in accordance with the TSTM-mould (Chapter 2.4.1).

The load-independent deformations were measured with 4 LVDT's in total (*Lokhorst, 2001*). Two LVDT's at each long side of the ADTM measured the load-independent deformation of a plain specimen over a length of 750 mm and of a reinforced specimen over the length of 800 mm.

3 Results of ADTM and TSTM-experiments

3.1 General remarks concerning the presentation of the results

Deformations are presented as strain by dividing the measured value by the measurement length of 750 mm in an unreinforced ADTM-specimen and by 800 mm in a reinforced one. Stress developments are presented as they were measured. This means nominal stresses σ_n are shown that are calculated by dividing the measured forces by the total cross section ($A_{\text{total}}=15000 \text{ mm}^2$ for HSC and $A_{\text{total}}=22500 \text{ mm}^2$ for NSC). For more graphs on experimental results than presented in this chapter reference is made to *Sule et al. (2000 and 2001a)*.

3.2 Effect of reinforcement on autogenous deformation

The general idea of the effect of reinforcing bars is that they provide inner restraint of concrete deformations. This was found in specimens cured isothermally at 20°C (Figure 3), 30°C and 40°C (Table 3). It was found that this restraining effect decreases with increasing temperature. This could be attributed to the complexity of the test execution where it is much more difficult to assure a constant temperature at higher temperatures than at room temperature.

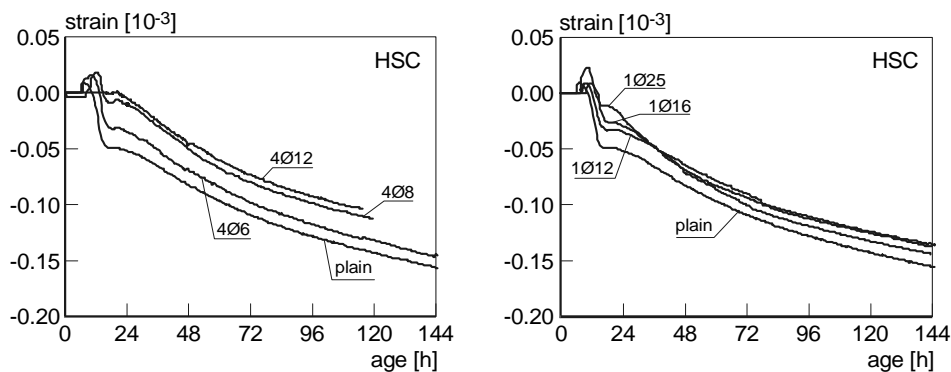


Figure 3: Effect of reinforcement percentage on autogenous deformations measured at 20°C curing temperature in specimens reinforced with four rebars (left) and one rebar (right).

Table 3: Autogenous deformations measured in reinforced HSC-specimens cured at different isothermal temperatures.

test name	concrete	T [°C]	$\epsilon_{total,plain}$ [10 ⁻³]	Reinforce ment	$\epsilon_{total,reif}$ [10 ⁻³]	Restraint [%]
T06R85i	HSC	20	0.199	4 Ø 6	0.163	18.1
T12R85i	HSC	20	0.184	1 Ø 12	0.145	21.2
T08A85i	HSC	20	0.213	4 Ø 8	0.132	38.0
T16A85i	HSC	20	0.185	1 Ø 16	0.153	17.3
T12A85i ^{*)}	HSC	20	0.182	4 Ø 12	0.167	8.2
T12A85ir	HSC	20	0.198	4 Ø 12	0.108	45.5
T25A85i	HSC	20	0.193	1 Ø 25	0.160	17.1
T08D85i ^{*)}	HSC	30	0.179	4 Ø 8	0.174	2.8
T16D85i	HSC	30	0.202	1 Ø 16	0.167	17.3
T16E85ir	HSC	40	0.205	1 Ø 16	0.190	7.3

^{*)} started too late

On the basis of the experiments performed at 20°C the following trends had been noticed: similar to hardening concrete, four rebars restrain autogenous deformations more than one rebar. This effect can be explained by a bigger specific surface of four rebars compared to one rebar representing the same reinforcement percentage. A bigger specific surface can directly be translated to a higher interaction between rebar and concrete. Comparing specimens with four rebars it was found that a higher reinforcement percentage (increasing specific surface) generates more restraint.

3.3 Stress development caused by restrained autogenous deformations

3.3.1 Effect of temperature on stress development

The stress development caused by restrained autogenous deformations was tested under different isothermal curing conditions (20°C, 30°C and 40°C). In the first test series none of the specimens cured at 20°C and 30°C cracked during the test period of 144 h.

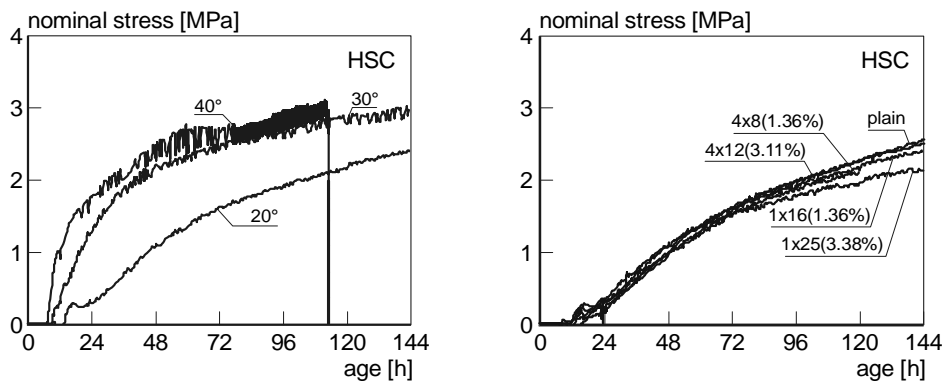


Figure 4: Effect of curing temperature (left) and reinforcement percentage (right) on stress development under isothermal curing at 20°C.

As the question arose if the specimens might crack at a later moment some isothermal experiments at 20°C were run for 240 h. In the end it appeared that the strength development was always ahead of the stress development and none of the specimens cracked.

Higher curing temperatures accelerate the hydration process. Consequently autogenous shrinkage develops faster and stresses develop faster in specimens subjected to higher curing temperatures. Figure 4 (left) illustrates that this was also found in the experiments performed here. At 40°C the autogenous deformations caused a stress development which exceeded the strength development during the test period (Sule & Van Breugel, 2001) leading to cracking of the specimen.

3.3.2 Effect of rebars on stress development

Rebars restrain free deformation of concrete. In a totally restrained specimen, however, rebars will only be activated if concrete cracks. Otherwise rebars cannot move with respect to concrete. The effect of reinforcing bars on the stress development is therefore of minor importance as long as the specimen does not crack and as long as there are no thermal effects leading to contractions or expansions of the rebar generating stresses.

In all isothermal experiments there were naturally no (or only little) thermal effects due to which the rebar deformed. When comparing the measured (nominal) stress curves of different reinforced specimens and plain specimens cured at 20°C (Figure 4, right) it was found that they were nearly the same.

3.4 Load-independent deformations under semi-adiabatic curing condition

3.4.1 Load-independent deformation of plain dummy specimens under semi-adiabatic curing

In the NSC as used in the experiments load-independent deformations could almost completely be deduced from temperature changes during the hydration process. In HSC there were thermal effects plus autogenous deformations due to the low w/c-ratio. Hydration-induced non-thermal deformations might have been occurred in the very early phase (Bjontegaard 1999). However, they were neglected as they did not affect the stress development. In Figure 5 the free deformations measured in NSC (left) and HSC (right) can be seen with scatter.

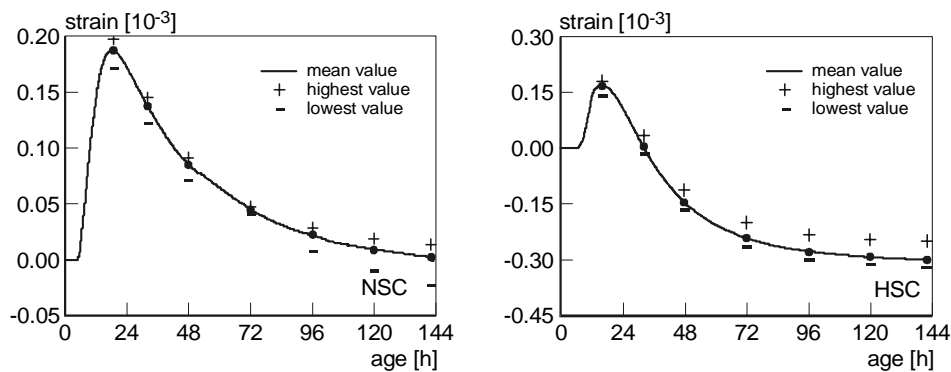


Figure 5: Mean value of load-independent deformation measured in all experiments with scatter on plain dummies in NSC (left) and HSC (right) cured semi-adiabatically.

3.4.2 Effect of reinforcement on load-independent deformations

Under semi-adiabatic curing conditions, concrete deformations are ruled by the hydration-induced thermal strains (NSC), or a combination of thermal strains and autogenous strains (HSC). As it is assumed that the thermal dilation coefficient (TDC) of rebars is about the same as for concrete

(except for the early phase, see *Sule 2003*) the influence of the rebars on the thermal deformation is expected to be relatively small.

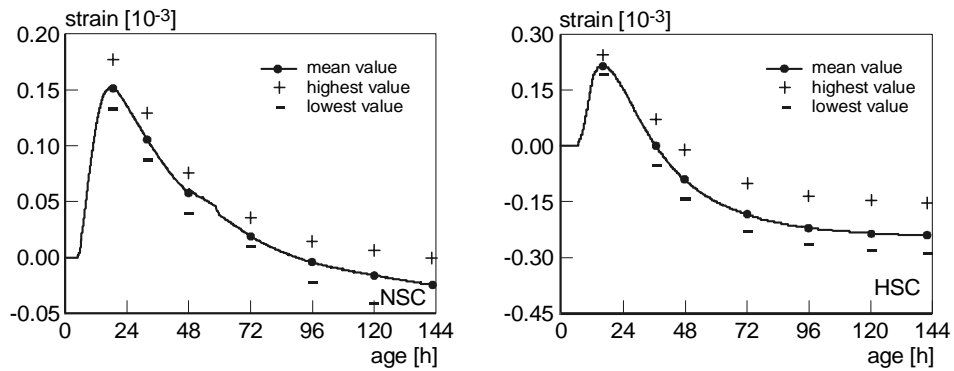


Figure 6: Mean value of free deformation measured in all experiments with scatter in reinforced dummies in NSC (left) HSC (right) cured semi-adiabatically.

Figure 6 shows the mean value with scatter of concrete strain measured in all reinforced specimens in NSC (left) and HSC (right) cured semi-adiabatically. As expected the total free deformation measured after 144 hours is in most reinforced specimens smaller than in plain specimens (compare Fig. 5, *Sule 2003*). On the basis of the few tests on NSC-specimens no clear trend could be found of the effect of reinforcement. The effect of reinforcement found in HSC cured semi-adiabatically is in accordance with what was found in HSC cured isothermally (see chapter 3.2).

3.5 Stress development under semi-adiabatic curing condition

3.5.1 Effect of reinforcement on stress development in NSC

As discussed earlier NSC undergoes almost only thermal deformations. Assuming that reinforcement steel has approximately the same TDC as concrete there should hardly be any effect of rebars on the stress development as long as the specimen is uncracked.

In Figure 7 it can be seen that compressive stresses are approximately the same in specimens with and without rebars. In Figure 7, left, the measurements in one experiment were started too late which is the reason why smaller compressive stresses were reached. In a test on a specimen with one rebar there was a problem with the control system keeping the specimen longer under compression than necessary. This test is not further mentioned.

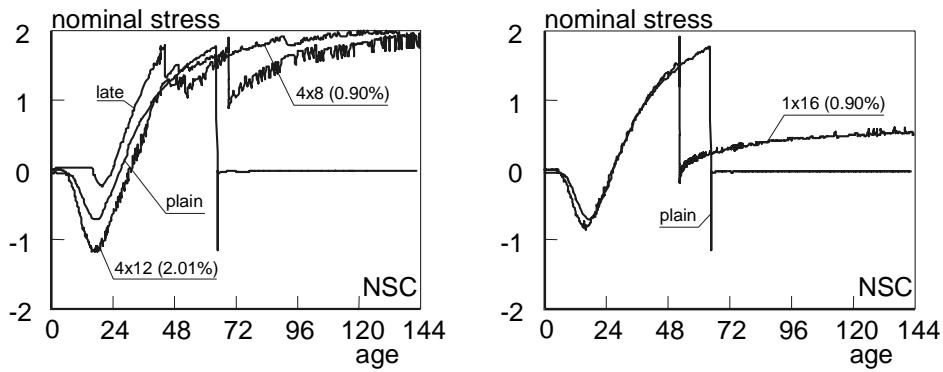


Figure 7: Development of nominal stresses in plain and reinforced specimens under semi-adiabatic curing in NSC, four rebars (left) and 1 rebar (right).

Comparing Figure 7, left and right, it appears that the reinforcement configuration has a major influence on the cracking behaviour of specimens at early age. Due to the formation of smaller cracks the formation of the first through-crack is postponed in the specimen with four rebars. The specimen reinforced with one rebar, on the other hand, cracks even earlier than the unreinforced specimen.

3.5.2 Effect of reinforcement on stress development in HSC

In Figure 8, left, it can be seen that a relatively low reinforcement percentage (0.75%) hardly influences the stress development in HSC. The nominal compressive and tensile stresses are slightly higher than in a plain specimen. However, the reinforced specimens crack at about the same moment as the plain specimen. In specimens with a higher reinforcement ratio (e.g. 1.36% in Figure 8, right) it can be observed that four rebars postpone the moment of through-cracking.

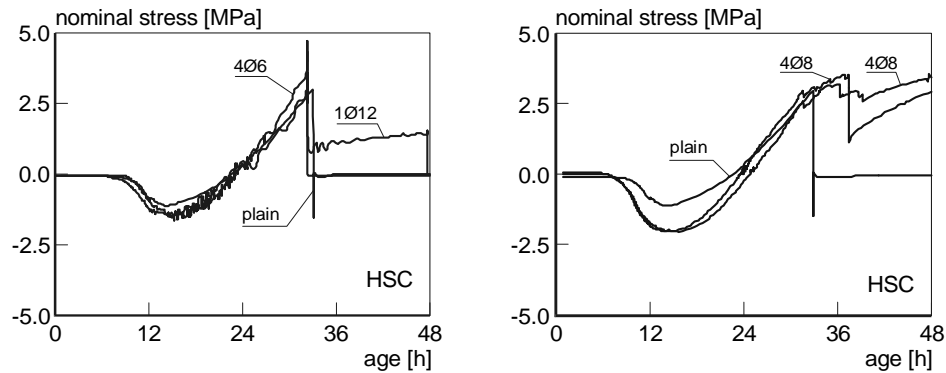


Figure 8: Effect of a low reinforcement ratio (0.75%, left) and medium reinforcement ratio (1.36%, right) on the stress development in HSC under semi-adiabatic curing condition.

When comparing the cracking behaviour of plain and reinforced specimens it strikes that the plain specimen cracked suddenly after about 33.5 h, whereas the stress-age curve of the specimens reinforced with four rebars “bent” before the first through-crack (Figure 8, right). After cracking, stresses built up in a reinforced specimen until the concrete tensile strength were reached again at a later moment and so on.

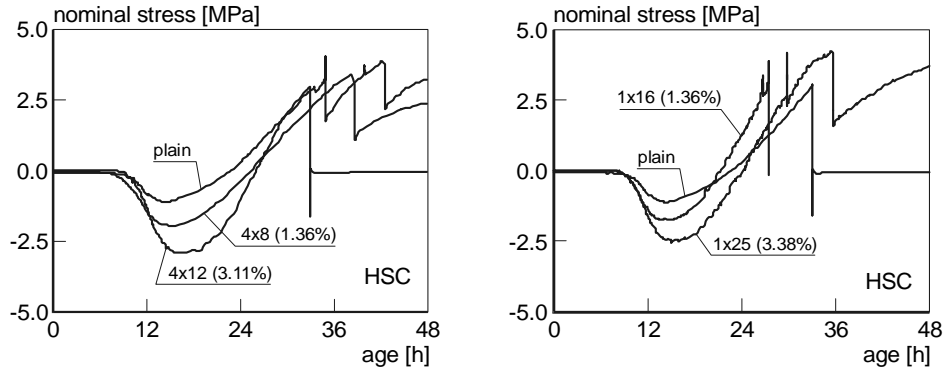


Figure 9: Effect of reinforcement configuration (four rebars, left and one rebar, right) on the stress development.

Figure 9 illustrates the effect of the reinforcement configuration at higher reinforcement ratios (1.36 %, 3.11 % and 3.38 %) in HSC. Comparing a plain specimen with differently reinforced specimens it can be seen that higher compressive stresses built up in reinforced specimens and the zero stress was passed later. With increasing reinforcement percentage the compressive stresses increased. Figure 9 (right) illustrates the stress developments of specimens reinforced with one rebar. It can be seen that the specimens with one rebar cracked even earlier or at the same age than the plain specimen.

4 Analyses of the experimental results

4.1 Influence of reinforcement on early-age cracking

The probability of cracking of concrete structures is often based on the development of stress-inducing deformations and concrete properties, i.e. the development of tensile stresses. The effect of reinforcement has been neglected up to now. For NSC structures this assumption is a reasonable approach.

However, in HSC, which is known to be prone to early-age cracking due to autogenous shrinkage, reinforcement was found to have a “strain enhancing effect” (Figure 9, left). As a result the probability of major through-cracks is reduced in reinforced HSC-elements.

The experimental results show that especially TSTM-specimens reinforced with four rebars postpone the occurrence of the first major crack (compare Figure 9, left). The deviating curve indicates that fine cracks are formed. This is confirmed by Figure 10, right (Sule 2003).

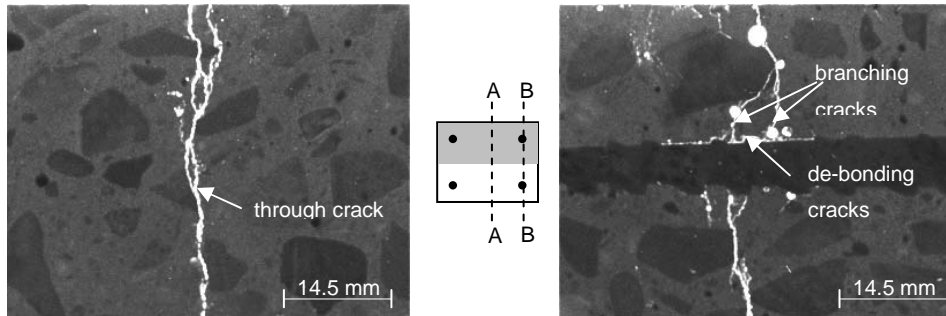


Figure 10: Crack pattern in the middle of the cross section (A-A, left) and in the vicinity of the rebars (B-B, right) of a reinforced HSC-specimen (4 Ø12) cured semi-adiabatically.

It is assumed that the formation of smaller cracks is initiated by a crack processing zone developing around the rebar. These smaller cracks increase the strain capacity of the TSTM-specimen before the occurrence of the first through-crack.

4.2 Defining a crack criterion

In order to define a crack criterion based on the data obtained in this research the 5%-fractile value is taken that can be calculated with a standard deviation of $0.09 \cdot f_{ctm,sp}$ ($0.74 \cdot f_{ctm,sp} - 1.64 \cdot 0.09 \cdot f_{ctm,sp}$) at $0.6 \cdot f_{ctm,sp}$. In practice a stress cracking criterion of $0.5 \cdot f_{ctm}$ which equals $0.45 \cdot f_{ctm,sp}$ (MC90) is often applied.

The stress/strain relation of plain HSC-specimens can be described with a linear diagram (Figure 12, left) where the cracking strain ε_{cr} is reached at $0.6 \cdot f_{ctm,sp}$. Then ε_{cr} can also be written as $\varepsilon_{cr,plain}$. For reinforced specimens a bilinear diagram (Figure 12, right) applies. In the bilinear diagram the elastic strain ε_{el} is reached at the first crack criterion $CC1$ given with the empiric Eq. 1 (Sule 2003).

$$\sigma_c > f_{ctm,sp} \cdot \left(\frac{c}{h} + \frac{d_s}{\omega} \right) \quad (1)$$

- c concrete cover
- h smallest side length of concrete prism surrounding one rebar (see Figure 11)
- d_s diameter of rebar
- ω reinforcement ratio

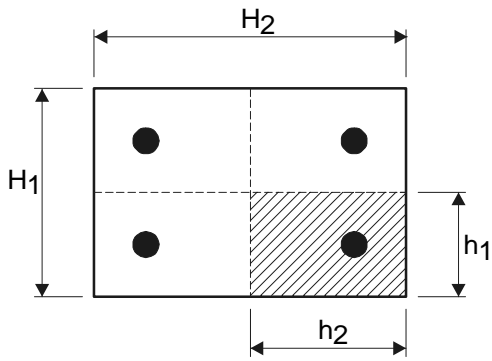


Figure 11: Definition of prism of concrete surrounding a reinforcing bar ($h_1 < h_2$ therefore is $h = h_1$).

The cracking strain of a reinforced specimen $\epsilon_{cr, reinforced}$ is reached at the second crack criterion $CC2$ ($0.6 f_{ctm, sp}$). If $\epsilon_{cr, plain}$ and $\epsilon_{cr, reinforced}$ are known the strain enhancing effect of reinforcement can be quantified with the help of a *strain enhancement factor* η_{cr} (Eq. 2):

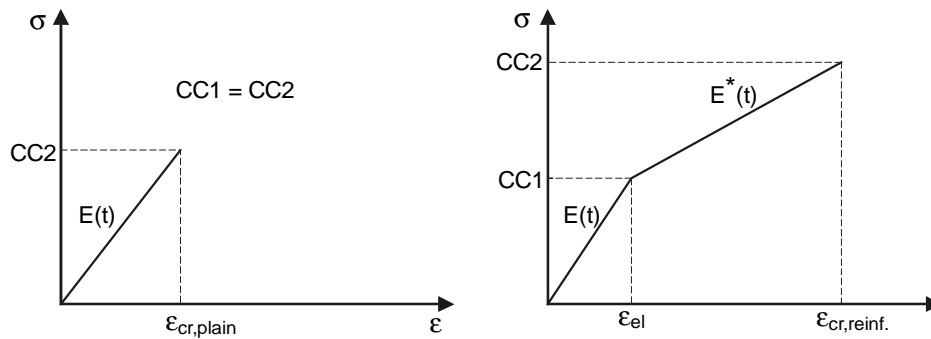


Figure 12: Model for stress/strain relation for plain (left) and reinforced (right) HSC-specimens for restrained load-independent deformations.

$$\eta_{cr} = \frac{\epsilon_{cr, reinforced}}{\epsilon_{cr, plain}} \quad (2)$$

Eq. [2] relates the cracking strain $\epsilon_{cr, reinforced}$ of a reinforced specimen to the cracking strain of a plain specimen $\epsilon_{cr, plain}$.

Table 4: Cracking strain of plain and reinforced HSC-specimen cured semi-adiabatically.

test	ω [%]	ϵ_{cr} [10 ⁻⁶]	mean value [10 ⁻⁶]	standard deviation [10 ⁻⁶]	mean value [10 ⁻⁶]	standard deviation [10 ⁻⁶]
plain	-	91	92	7	92	7
plain	-	92				
4Ø8	1.36	161				
4Ø8	1.36	160	170	16		
4Ø8	1.36	188			170	20
4Ø12	3.11	168				
4Ø12	3.11	198	169	28		
4Ø12	3.11	142				

Table 4 presents the cracking strain measured in plain specimens and specimens reinforced with four rebars. The presence of reinforcement appears to have a substantial impact on the strain at which the first through-crack occurs. The figures also indicate that the reinforcement ratio, i.e. whether it is 1.36% or 3.11%, has only a minor influence on the cracking strain. With the values summarised in Table 4 it can be seen that the strain capacity of specimens reinforced with four rebars is on average 1.85 times higher than the strain capacity of plain specimens.

4.3 Development of bond stress at early age

On the basis of the experimental data obtained in pull-out tests (Sule 2003) on young concrete, a bond stress-slip relation has been formulated as a function of the degree of hydration. For this relation a power function (Eq. 3) has been chosen. This choice was made in order to make it possible to use the analytical method of Noakowski (1978) for calculating crack widths and the required minimum reinforcement ratio.

The experimental results of pull-out tests could be well described with Eq. 4 that appeared to be applicable for both NSC and HSC. The parameters a and b only depend on the critical degree of hydration α_0 and the mean value of cube compressive strength as the function of the degree of hydration, $f_{cm}(\alpha)$. With $a = 4.8 \cdot \alpha_0 \cdot f_{cm}(\alpha)$ and $b = 3.6 \cdot \alpha_0$, the calculated theoretical crack width (Eq. 5) in NSC was almost identical to the one based on formula from earlier research. For HSC, however, smaller crack widths were calculated. This seems reasonable as the bond between HSC and rebar is better than in NSC. In order to validate the author's equation more experiments have to be performed with different types of concrete.

$$\tau_b = a \cdot \Delta^b \quad (3)$$

$$\tau_b(\Delta, \alpha) = 4.8 \cdot \alpha_0 \cdot f_{cm}(\alpha) \cdot \Delta^{3.6 \cdot \alpha_0} \quad (4)$$

$$w_{cr} = 2 \cdot \Delta_{cr} = 2 \left[\frac{1+b}{8} \cdot \frac{d_s}{a \cdot E_s} \cdot \frac{\sigma_{s,cr}^2}{(1+n\omega)} \right]^{\frac{1}{1+b}} \quad (5)$$

5 Example: Early-age cracking on a HSC cantilever bridge (2nd Stichtse Brug)

5.1 Calculating crack width and number of cracks due to load-independent deformations

In an earlier project *Gall (1997)* calculated the crack width and required reinforcement for the deck of an on site cast free cantilever bridge (2nd Stichtse Brug) subjected to shrinkage and temperature effects. In order to verify his calculations he compared his results with crack widths measured on site. A comparison of the author's experimental results and *Gall's* work is reasonable as the investigated HSC-mixture was the same in both cases.

Figure 13 shows the calculated concrete stress development according to *Gall*. The restraint of the deformations by the previously cast segment has been calculated with the FE-package DIANA and is 50 % (Figure 13, right, *Van der Veen et. al., 1996*). The mean value of the calculated moment of cracking t_{cr} is after 58 hours. In practice cracking was observed between 52 and 71 hours. Although the difference between calculated and measured value is not extreme, it has to be noticed that a difference of several hours in the time until cracking corresponds to a considerable difference in the allowable temperature or strain difference.

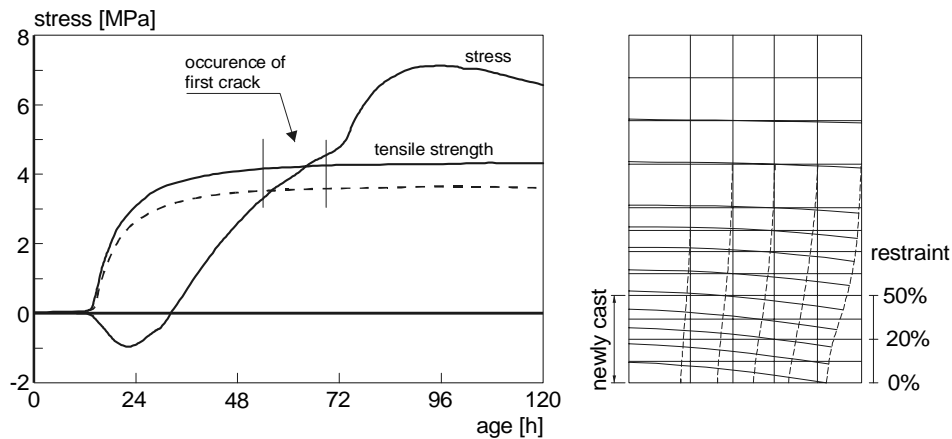


Figure 13: Calculated stress development according to *Gall (1997)* and restraint of calculated deformations of a newly cast segment according to *Van der Veen et. al. (1996)*.

Table 5 summarizes the parameters calculated by *Gall* for determining the crack width and the number of cracks. In order to calculate crack widths *Gall* used Eq. 5 developed by *Noakowski (1978)*. The number of cracks were calculated with Eq. 6, assuming that the temperature drop ΔT after the first crack causes the dominant part of the deformation. For this reason autogenous shrinkage is not accounted for. For the number of cracks it holds:

$$n_{crack} = \frac{\Delta T \cdot \alpha_{cT} \cdot l_{crack}}{w_{cr}} \quad (6)$$

ΔT	temperature drop after the first crack
α_{cT}	thermal dilation coefficient of concrete
l_{crack}	considered length where cracks occur
w_{cr}	average crack width at instance of cracking

Table 5: Parameters calculated by *Gall* (1997).

T_{cr} [h]	$f_{ctm}(t_{cr})$ [Mpa]	$\sigma_{c,cr}$ [Mpa]	$E(t_{cr})$ [Mpa]	ΔT [K]
58	3.54	$0.85 \cdot f_{ctm}(t_{cr})$	39428	23

5.2 Comparing calculation results and observation on site

For a reinforcement percentage of 1.25%, realized with \varnothing 20-120, *Gall* calculates a mean crack width of 0.14 mm and a maximum crack width of 0.18 mm. The maximum measured crack width was 0.17 mm with a smaller deviation as calculated. These values are in good accordance to each other. Using the same parameters as *Gall* did, the average crack width calculated with Eq. 5 was 0.12 mm using the parameters a and b from Eq. 4. Then the maximum crack width is calculated to $1.3 \cdot 0.12 \text{ mm} = 0.16 \text{ mm}$ (*Noakowski 1978*).

On site 7 cracks were counted in contrast to 13 cracks that were calculated by *Gall* and 11 calculated by using the parameters a and b from Eq.4 and $\sigma_{c,cr} = 4.5 \text{ Mpa}$. This difference could not be explained by *Gall*. However, it has to be kept in mind that Eq. 6 is only a rough approximation especially if the state of crack formation has not been terminated. Then the concrete strain between cracks is not taken into account. Another reason might be that some of the calculated cracks might be not visible on the surface due to the crack distributing effect of the rebars.

5.3 Comparing calculation to experimental results

In practice it is still a problem how to quantify fine cracks. By comparing the calculated number of cracks with the counted number of cracks (11 vs. 7 and 13 vs. 7), it can be found that the strain capacity of the flange is 1.57 to 1.86 times larger than calculated. This is the same range of the effect of reinforcement on the cracking behaviour that was found in the TSTM-experiments (chapter 4.2). Hence, it can be concluded that in this respect the results from the TSTM-experiments are in close agreement with observations on site and constitute a good explanation for the latter phenomenon.

6 Conclusion

Due to the elaborated experimental set-up and the long testing period (at least one week per test) only limited test data could be generated. Based on this test data, however, it was found that the reinforcement configuration had more influence on the moment of cracking than the reinforcement ratio. Generally, the effect of reinforcement can be considered as advantageous. For practice this means that less cooling or fewer dilation joints are needed in order to prevent through-cracking at early-age. Or, in other words, the probability of cracking in highly reinforced structures is lower than has been estimated in calculations where the effect of reinforcement is completely ignored. For quantifying the effect of reinforcement on the stress development due to restrained load-independent deformations, a "strain enhancement factor" has been introduced. From the experiments with HSC-specimens reinforced with four rebars this factor reached a mean value of 1.85. For practice this means that strains calculated on the basis of a stress criterion are short selling reinforced HSC as its strain capacity is 85% higher than the plain HSC strain. Summing up, the effect of reinforcement that has been found (pronouncedly in HSC) justifies to reduce the reinforcement percentage for early-age crack control up to 10% in HSC.

7 Acknowledgement

The assistance of the laboratory technicians of Stevin laboratory is gratefully acknowledged. A special thanks goes to Mr A. van Rhijn for performing the experiments. This project could be realised thanks to the financial support of the Dutch Technology Foundation (STW) and the Ministry of Transport, Public Works and Water Management (RWS).

Literature

- Emborg, M., Bernander, S. (1994), *Assessment of risk of thermal cracking in hardening concrete*, ASCE Journal of Structural Engineering, Vol. 120, No. 10, pp. 2893-2912.
- Koenders, E.A.B. (1997), *Simulation of Volume Changes in Hardening Cement-Based Materials*, Doctoral Thesis, TU Delft.
- Lokhorst, S.J., (2001), first print 1998, *Deformational behaviour of concrete influenced by hydration related changes of the microstructure*, Report 25.5-99-05, TU Delft.
- MC90 (1993), *CEB-FIB Model Code 1990 for concrete structures*, CEB Bulletin d'Information, No. 213/214, Comité Euro International du Béton, Lausanne, pp. 437.
- Noakowski, P. (1978), *Die Bewehrung von Stahlbetonbauteilen bei Zwangsbeanspruchung infolge Temperatur*, Deutscher Ausschuss für Stahlbeton, Heft 296.

- Sule, M., Van Breugel, K., Van Rhijn, A. (2000), *Experimental research on the effect of reinforcement on cracking in early age concrete due to temperature effects and autogenous shrinkage*, Research Report, 25.5-00-09, TU Delft.
- Sule, M., Van Breugel, K., Van Rhijn, A. (2001a), *Second experimental series on the effect of reinforcement on cracking in early age concrete due to temperature effects and autogenous shrinkage*, Research Report, 25.5-00-09, TU Delft.
- Sule, M. & Van Breugel, K. (2001), *Possibilities of reinforcement to control cracking caused by autogenous shrinkage in view of designing durable concrete structures*, CONCREEP 6, Boston.
- Sule, M. & Van der Veen, C (2002), *Development of bond between reinforcement steel and early age concrete*, Bond in concrete – from research to standards, 2002, Budapest.
- Sule, M. (2003), *Effect of reinforcement on early-age cracking in high strength concrete*, Doctoral Thesis, TU Delft.